RESEARCH PROJECTS

STUDENTS OF THE DEPARTMENT OF MECHANICAL ENGINEERING

modéliser
simuler
réaliser
expérime
communiquer

département
génie
mécanique

2021-2022

ABSTRACT
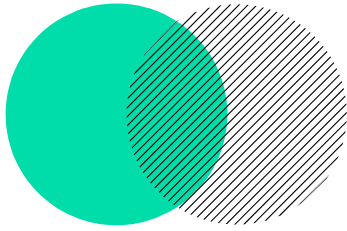
Influence of collagen fiber organization on the thermo-response of human connective tissues

C. DRAME-MAIGNE , E. FOULATIER, E. BUDYN

TER M1 2021-2022 Final
defence of research projects

école
normale
supérieure
paris—saclay

Influence of collagen fiber organization on the thermo-mechanical response of human connective tissues

C. Dramé-Maigné[*], E. Foulatier[†], E. Budyn[◇]

Department of Mechanical Engineering
Ecole Normale Supérieure Paris-Saclay
University Paris-Saclay
4, avenue des Sciences, 91190 Gif-Sur-Yvette, France
e-mail: [*] charles.drame-maigne@ens-paris-saclay.fr ; [†] elise.foulatier@ens-paris-saclay.fr ;
[◇] ebudyn@ens-paris-saclay.fr

KEYWORDS: bone; osteon; collagen fiber; finite element method.

ABSTRACT

Motivations

Human bone continuously repairs defects in which new bone is formed by mesenchymal stem cells (MSCs) that differentiate into osteoblasts and later osteocytes. However, bone is unable to repair very large defects in particular following massive trauma or surgeries such as a cancer resection leading to significant cost on the healthcare system. Therefore, it is essential to gain insight on mechanisms regulating bone formation in order to improve current therapeutics. From correlation between high resolution images and the analysis of the local tissue loading, researchers have shown that the orientation of the mineralized collagen fibers is influenced by the direction of mechanical loading [1]. Stockhausen [2] modeled the mechanical micro-environment around ostecyte lacunae with respect to the orientation of the collagen fibers after measurements using FTIR (Fourier Transform Infra Red). Dark osteons in which collagen fibers are aligned with their central axes and bright osteons in which collagen fibers have an offset direction with respect to the central axes displayed different mechanical behaviors.

The purpose of this study is to understand the way collagen fibers respond to an impact on the bone depending on their geometrical structure. Previous research have established a numerical method to create a 3D geometry of biological elements. This method will be extended to collagen fibers in order to carry out mechanical simulations on the whole model.

Methods

We propose to construct a unit cell volume containing two compartments with collagen fibers of varying orientations. The unit cell volume is located in the vicinity of an osteocyte cytoplasmic process. The 3D geometry of the collagen fibers of diameter equal to $125nm$ is considered first as an idealized 3D helix of diameter equal to $150\mu m$ corresponding to the average diameter of an Haversian lamella. The axial spacing between each helix has been measured in TEM observations (Transmission Electron Microscopy) [3]. Along the
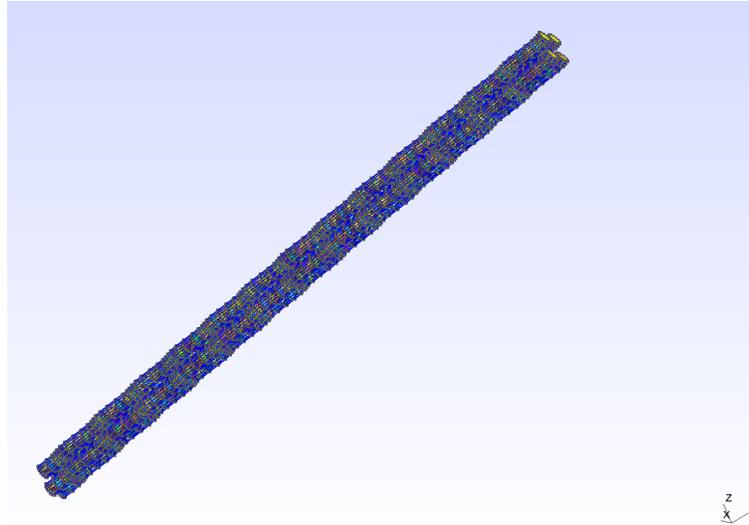
Figure 1: Morphology and mesh generation of four collagen fibers in GMSH

helix, the collagen fibers display a characteristic sinusoïdal morphology of amplitude equal of $42nm$ that is included in the model in Fig. 1. Finally, the unit cell is centered around a cytoplasmic process based on a finite element model using orphan geometry measured in fluorescent confocal microscopy observations [4].

Results

Tensile and compressive tests of the unit cells containing collagen fibers of different orientations are implemented. Two orientations of study have been privileged: collagen fibers with an orientation of 45° with respect to the osteonal central axis representing bright osteons and collagen fibers with an orientation of 80° with respect to the osteonal central axis representing dark osteons.

REFERENCES

[1] J. G. Skedros, C. J. Kiser, K. E. Keenan and S. C. Thomas, *Analysis of osteon morphotype scoring schemes for interpreting load history: evaluation in the chimpanzee femur*, J. Anat., v. 218, p. 48099, 2011.

[2] K. E. Stockhausen, M. Qwamizadeh, E. M. Wlfel, H. Hemmatian, I. A. K. Fiedler, S. Flenner, E. Longo, M. Amling, I. Greving, R. O. Ritchie, F. N. Schmidt and B. Busse, *Collagen Fiber Orientation Is Coupled with Specific Nano-Compositional Patterns in Dark and Bright Osteons Modulating Their Biomechanical Properties*, ACS Nano, v. 15, p. 455?467, 2021

[3] N. Reznikov, R. Shahar, S. Weiner, *Three-dimensional structure of human lamellar bone: The presence of two different materials and new insights into the hierarchical organization*, Bone, v. 59, p. 9304, 2014.

[4] E. Budyn, N. Gaci, S. Sanders, M. Bensidhoum, E. Schmidt, B. Cinquin, P. Tauc, H. Petite, *Human Stem Cells Derived Osteocytes in Bone-on-Chip*, MRS Advance, v. 3(36), p. 1443-1455, 2018, doi.org/10.1557/adv.2018.278
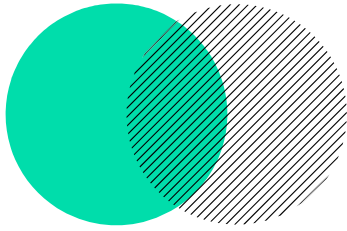
Design of textured toughened interfaces through dissipation mechanisms at different length scales

V. FOUQUET   L. MABILEAU   F. DAGHIA

école
normale
supérieure
paris—saclay

Design of textured toughened interfaces through dissipation mechanisms at different length scales

Vivien Fouquet[*], **Lucas Mabileau**[*], **Federica Daghia**[*,◊]

[*] Department of Mechanical Engineering
4 avenue des sciences, 91190, Gif-Sur-Yvette
e-mail: {vivien.fouquet,lucas.mabileau}@ens-paris-saclay.fr

[◊] Université Paris-Saclay, CentraleSupélec, ENS Paris-Saclay, CNRS
LMPS - Laboratoire de Mécanique Paris-Saclay, 91190, Gif-sur-Yvette, France.
e-mail: federica.daghia@ens-paris-saclay.fr

KEYWORDS: Delaminating; Cohesive zone model; Damaging interfaces; Toughening strategy; Snap-back instabilities.

ABSTRACT

General Information

The composites with long and oriented fibres and polymer matrices are increasingly developed in sectors like transports. The gluing process to create an assembly is increasingly used in those sectors. However, the area where the two materials are glued is a weak plane of the structure, therefore cracks can happen. The search for a solution to improve the toughness of these areas is important because the behaviour of the glue is very fragile. This study aims to understand the phenomena of bridging and bounding that are present in the textured interface between fibres and polymer matrix to make the propagation of the failure more gradual.

Methods

To begin the study of the textured interface between the substrate and the glue, a model based of the DCB (double cantilever beam) with textured interface is created. These interfaces are composed from a pattern of two cohesive zone models which creates the bridging phenomenon (creation of ligaments between the two substrates illustrated on Figure 1) [1, 2]. The cohesive zone model is defined by a stiffness K, a maximal stress σ_0, the energy release rate G_c. The cohesive length λ links these quantities [1]. It is computed with a dissipation-driven arc-length algorithm in order to see the phenomena of snap-back instabilities. In this model the glue does not have a plasticity law implemented, then damages in glue are not computed.
A second approach is made using a complex cohesive zone which is constructed using two simple triangular cohesive models combined in parallel to homogenized the previous DCB test. It is modeled with that cohesive law between the two substrates. The use of two of them enables to have different cohesive length. The first has a short cohesive length and the second a long one. The combination of the two interfaces allows the model to have two different mechanisms of energy dissipation [3]. The goal of this approach is to fit the model to the experimental results [2] and the previous numerical test and then understand the impact of the different parameters of the long-scale interface on the global result [3].

Results

Figure 1 illustrates the non-linearity issue of the calculation with some snap-back instabilities for the first model. They appear when the weak interface is broken and the load is transferred on a second interface. The texturing shows a gradual crack propagation.
The result of the second model of the parametric analysis on max stress of the long-scale interface is shown on Figure 2. The bounds on the curve represent the theoretical DCB curve using fracture mechanics for the G_c of the first interface and the sum of the G_c of both interfaces. The maximal stress of the second interface influences the rapidity that the second part of the curve reaches the upper bound.
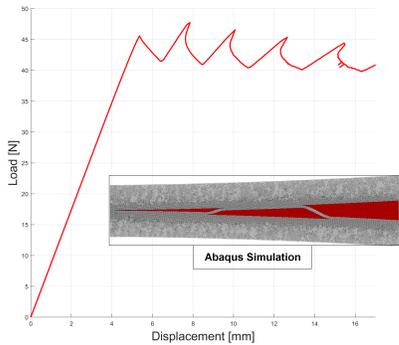

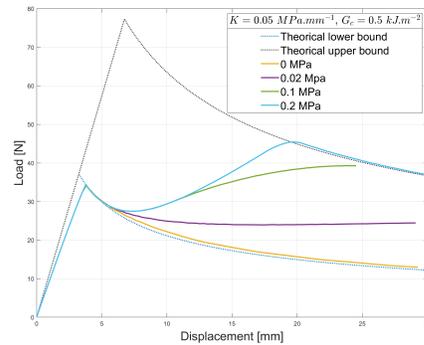**Figure 1**: Load-displacement curve of the textured DCB essay

Figure 2: Load-displacement curve with different values of the maximal stress of the long scale interface

Conclusion and perspectives

Contrary to the homogeneous behaviour, the textured modeling is still unstable with the appearance of snap-backs. The behaviour needs to be more gradual and to generate more dissipation. Moreover, the understanding of the local behavior of the textured interface would be necessary in order to make the connection with the model with complexe cohesive zones.

REFERENCES

[1] G. Bao, Z. Suo, Remarks on Crack-Bridging Concepts, Applied Mechanics Reviews 45 (8) (1992) 355–366.

[2] R. Tao, X. Li, A. Yudhanto, M. Alfano, G. Lubineau, On controlling interfacial heterogeneity to trigger bridging in secondary bonded composite joints: An efficient strategy to introduce crack-arrest features, Composites Science and Technology 188 (2020) 107964.

[3] R. Sills, M. Thouless, Cohesive-length scales for damage and toughening mechanisms, International Journal of Solids and Structures 55 (2015) 32–43.
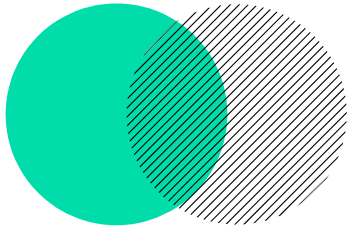
Instrumentation of a Cyber-physic system for the identification by hybrid automata

G. FLINOIS, V. PERRET, M. ROYER

Instrumentation of a Cyber-physic system for the identification by hybrid automata

Guillame Flinois, Vincent Perret, Maxime Royer

Department of mechanical engineering (DGM)
ENS Paris-Saclay, 4 Av. des Sciences, 91190 Gif-sur-Yvette, France
e-mail: {maxime.royer, vincent.perret, guillaume.flinois}@ens-paris-saclay.fr

KEYWORDS: Distributed data acquisition; industrial field buses; Synchronisation of time series.

ABSTRACT

General Context
An aim in modern production industry is the creation of numerical twin models to simulate the whole lifespan of a product, taking into account features such as its ageing and defects. Thus, ongoing research study the behaviour of discrete events and continuous variable systems. Our project more specifically focuses on data acquisition, whether they be discrete or continuous, without interfering with the systems. This effectively enables precise measures with little impact on the device. We developed our method on an educational machine provided by Schneider Electric (the *Xylophonis*), which shares its components with other real industrial devices from the company.

Methods
We divided the data we were looking for in two main types, discrete data found in field buses and analog data (current through a actuator for example). This brings a plurality of temporal bases for the acquisitions which later need to be synchronised. Thus, we decided to organise our method in three steps.
Raw data acquisition: First of all, we needed to acquire data. On the one hand, we were looking for the kinematic, kinetic and dynamic states of the moving tray; on the other hand the state of the firing pin. The state of the firing pin was acquired thanks to a Analogue to Digital converter plugged to a computer. All the information on the moving tray were internally communicated via a CANbus which we thus spied on using a micro-controller card equipped with the proper peripherals.
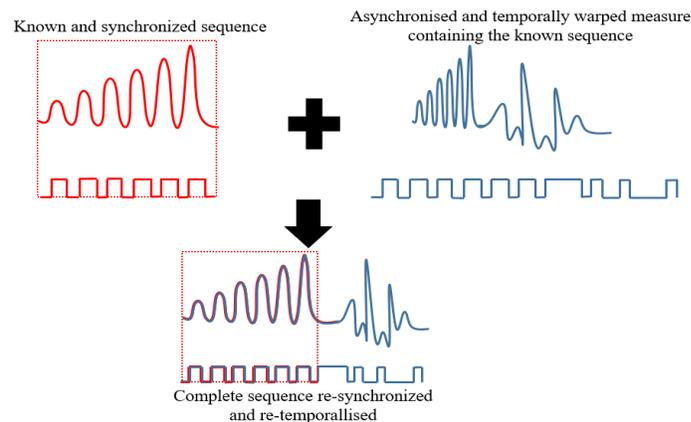**Field bus decoding:** The protocol used in the *Xylophonis* is CANopen, thus based on CANbus infrastructure. It is with an object library which allows communication between a variator, the motors and diverse sensors. Each object has its own binary address. Amongst them, one conveys the position and the velocity of the tray. Therefore, we built a Python program to analyse the recovered data coming from our system. It was made to decrypt the CANopen data set to extract information we need.
Clock synchronisation: Having collected data, we need to make it coherent both temporally and in size. We identified a predefined sequence (called common) on which all the acquisition methods bore at least once the same information (hitting the limit switch in our case in the zero point of the machine), allowing us to synchronise our data. We then created an easily recognisable sequenced that could be fired easily whilst the machine was

running. We played this "Starting of the measure" sequence after the "common" sequence, in order to have a record of it being synchronised. Using the first sequence we matched the second on the time dimension of our various measuring systems, and using the second that we stored, we can match it again at any point of the activity of the machine by doing this same recognisable sequence. To do this matching of the same sequences we use auto-correlation [1] on upsampled and downsampled [2][3] versions of our signal in order to have enough values to find a precise enough value for the delay for further use of identification.

Results

The figure below shows the clock synchronisation on a measure with the help of the sequence we created. They contain the same pattern but timed differently, the synchronisation allows with correlation to time precisely the measures.

Known and synchronized sequence

Asynchronised and temporally warped measure
containing the known sequence

Complete sequence re-synchronized
and re-temporallised

Further work

During the study, we did not taking into account mechanical actions in the system due to the absence of heavy item in it. In real industrial machines, we also need to measure these data with a non-intrusive way to get a complete model. It could be possible using load monitoring based on deep neural network and differential current [4]. Other types of data would require other types of measuring systems and thus requires further work.

REFERENCES

[1] W. Menke et J. Menke. "9 - Detecting correlations among data" *Environmental Data Analysis with MatLab*. Boston: Elsevier, 2012.

[2] T. F. Kraemer. *A study of time series interpolation and decimation with signal processing applications*. Master Thesis, 1978.

[3] Y. Guo, L. Wang, and A. Kareem. *Interpolation of Discrete-Time Series*, J. Eng. Mech., juin 2020

[4] Shaokang Ding, Hongwei Zhu. *Non-Intrusive Load Monitoring based on Deep Neural Network and Differential Current*, Hangzhou, China, 2020
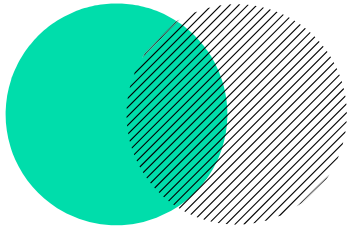
Exploratory Tests on a Hopkinson Device with 4 Tension Bars

E. LE PRIOL, T. RAVERDY, B. DURAND

école
normale
supérieure
paris—saclay

Exploratory Tests on a Hopkinson Device with 4 Tension Bars

E. Le Priol*, T. Raverdy†, B. Durand⋄

* Mechanical engineering department
Ecole Normale Superieure Paris Saclay
4 avenue des Sciences, 91190 Gif-Sur-Yvette, France
e-mail: etienne.le_priol@ens-paris-saclay.fr, thomas.raverdy@ens-paris-saclay.fr

KEYWORDS: Hopkinson bars; material dynamics; bi-axial tension, digital image correlation.

ABSTRACT

General Information

In the industry, the dynamic characterization of materials is vital knowledge in order to comprehend the mechanical behavior of structures under shock stresses. The split Hopkinson pressure bars, initially designed for characterising the mechanical response of materials under dynamic uni-axial-compression loads, can also be used for dynamic uni-axial-tension loads. Moreover, realistic loads often involve multiple directions of load. Therefore, researchers focus on the making of a bi-axial dynamic tension device [1], using Hopkinson bars.

Using four sliding surfaces, the setup allows the transformation of an impact into a bi-axial load using a traditional Hopkinson bar setup. Strain is measured both on the input and output on each of the four bars with gauges, and the forces and displacements applied to the interfaces between the bars and the sample are identified through the theory of Lagrange. High-speed imaging using digital image correlation is also used to obtain the displacement field on the area of interest of the sample.
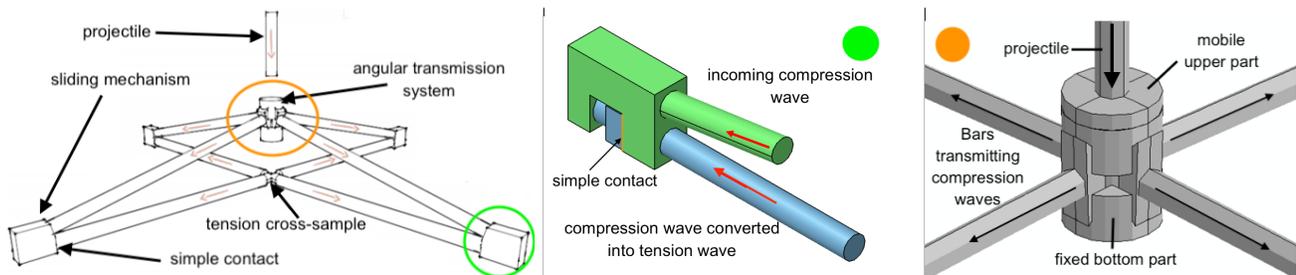
Figure 1: Detail and functioning of the device

Previous work on the bi-axial-Hopkinson bar device proved the validity of dynamic bi-axial compression test results. For bi-axial-tension, the final design was developped on CATIA comprehending an inertia continuous to the one of the Hopkinson bars while being able to clamp the tested part without mechanical clearance. The machining of the jaws being part of the project, the material used is the same maraging steel as the Hopkinson bars. This choice of design was done in order to apply tension strain to the tested part only, thus maximizing the stiffness of the jaws and other parts of the device.

Results

After multiple experiments, the accuracy of the results was linked to the precision of the adjustment of the device's mechanism, minimizing every clearance. Otherwise, clearances lead to mechanical-lag, resulting in non-conclusive results due to noise.

Figure 2: CATIA visualization of the tension mechanism and actual device

Hence, with the device adjusted at the best possible, multiple experiments were conducted in order to prove the feasibility of a bi-axial tension dynamic instrumented test.

The data processing was realised by a Python program. This handling program extracts data from the gauges which allows to determine the forces and displacement at the bar-sample interfaces.
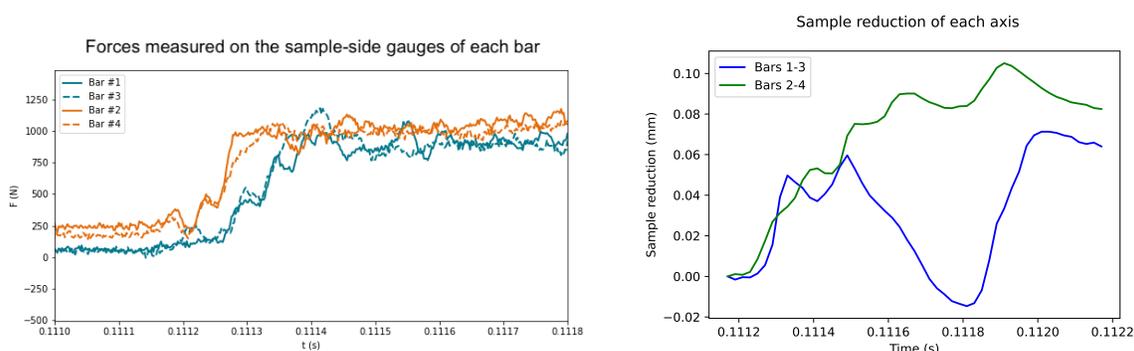

Figure 3: Gauges' and image correlation's displacement field

Firstly, despite the slight lag between both axis (1-3 and 2-4), the forces measured by gauges show simultaneous loads on both axis at $t = 0.1112s$ approximately.
Secondly, the results of the image correlation present a distinct raise of sample reduction at $t = 0.1112s$ on both bars.
Therefore, the previous graphics confirm the bi-axial behaviour of the Hopkinson tension test thanks to the displacement field of both axis, showing simultaneous action-effect on both image correlation and forces measured by gauges.

Further work

In further work, experimental dynamic uni-axial results will be linked to dynamic bi-axial results in order to confront the experimental model to the Von Mises theory. In order to achieve this connection, finite element analysis software like Abaqus will be used in order recreate bi-axial results using the material's mechanical law deduced from simple tension measurements to build a comparison.

REFERENCES

[1] Bastien Durand, Pierre Quillery, Ahmed Zouari, Han Zhao. *Exploratory Tests on a Biaxial Compression Hopkinson Bar Set-up.* Experimental Mechanics, Society for Experimental Mechanics, 2020, 10.1007/s11340-020-00665-7 . hal-02963087
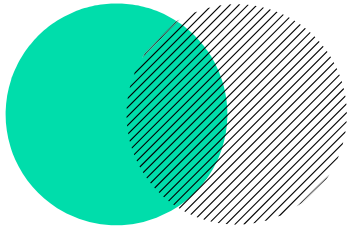
Creation of a benchmarking library for the identification of cyber-physical systems to hybrid models

G LEMBREZ, A. CALAME

Creation of a benchmarking library for the identification of cyber-physical systems to hybrid models

G. Lembrez[*], A. Calame[†]

[*][†] Département de génie mécanique
Ecole Normale Supérieure Paris-saclay
4, avenue des Sciences 91190 Gif-sur-Yvette
e-mail: [*] gabin.lembrez@ens-paris-saclay.fr, [†] alvi.calame@ens-paris-saclay.fr

Supervised by Gregory Faraut

KEYWORDS: hybrid automata; cyber-physical system; identification.

ABSTRACT

Introduction and context

Cyber-physical systems are systems in which software elements are in control of physical entities. On the occurrence of discrete events, these systems can switch between states in which their behaviour is continuous. Most industrial systems fall under this characterisation, rendering critical the ability to identify them to manageable models. However, the development of an identification method requires a collection of training examples. The hybrid automaton formalism allows for a systematic approach to the design of cyber-physical systems. The aim of this study is to provide a benchmarking library for the identification techniques of cyber-physical systems to this model.

Methods

All the simulations have been conducted using the stateflow environment from MATLAB. A preliminary work is dedicated to the definition of the formalism used with respect to the two formalism of reference in the field. In fact, while Stateflow semantic is based on Harel's statecharts model [1], it is enriched to take into account the concepts of location and flow from hybrid automata theory developed in [2, 4].

The main part of this work is dedicated to the gathering and simulation of a collection of examples from literature. The selected examples fall under two categories. First, most models are automata developed in previous work. However, we also implemented the hybrid automaton model of real cyber-physical systems.

Finally, to facilitate the selection of an example in the collection, a set of criteria has to be decided. To provide these features, we examined the hypothesis of each model with respect to the formalism as well as the characteristics of the output signals.

Results

Our work resulted in the constitution of a benchmark which can be used to assess the performances of identification methods. Each developed model is provided with a set of
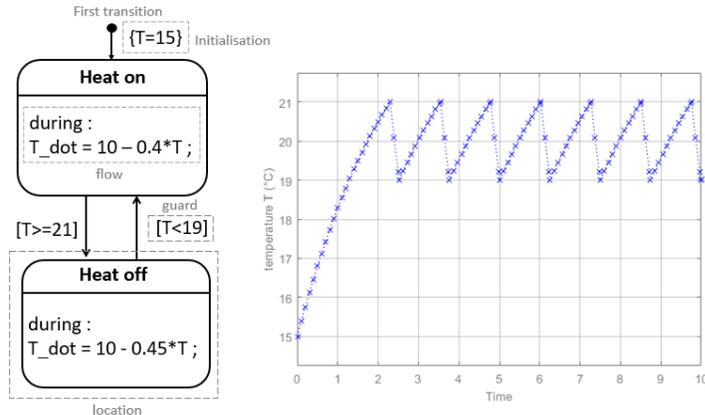
Figure 1: Automaton used for an identification process

hyperparameters and the most complex ones can be fed. The output data is post-treated to be ready to be used as input for an identification algorithm such as [3]. In addition, the output data can be manipulated at will by tuning sampling rates and adding noise. Figure 1 provides an example of an utilisation of the benchmark on a simple model of a two-states thermostat.

The set of examples provided covers a wide range of behaviour with varying degrees of complexity from an identification perspective. We selected 6 criteria to be able to chose an example in the benchmark. The most significant features are the ability of the automaton to observe time series in input or the presence of discontinuities in the output data due to affectation of variables within transitions.

Future work

Further work is needed to broaden the data set. In addition, a formal definition of classes of automaton based on the classes of its differential equations would facilitate the choice of an example from the list.

REFERENCES

[1] David Harel. Statecharts: a visual formalism for complex systems. *Science of Computer Programming*, 8(3):231–274, June 1987.

[2] Thomas A. Henzinger. The Theory of Hybrid Automata. In M. Kemal Inan and Robert P. Kurshan, editors, *Verification of Digital and Hybrid Systems*, NATO ASI Series, pages 265–292. Springer, Berlin, Heidelberg, 2000.

[3] Yan Monier. Cyber-physical system identification in the context of digital twin conception. 2021.

[4] Jean-François Raskin. An Introduction to Hybrid Automata. In Dimitrios Hristu-Varsakelis and William S. Levine, editors, *Handbook of Networked and Embedded Control Systems*, Control Engineering, pages 491–517. Birkhäuser, Boston, MA, 2005.
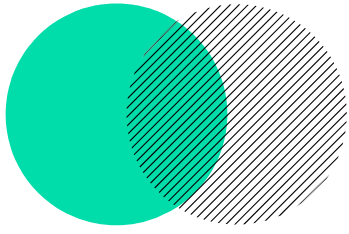
Ice detection based on multi-functional structure concept

T.CHASTEL, E.MARQUIS, T.REY, H.RAFIK, F.FEYEL

Ice detection based on multi-functional structure concept

Chastel Timothée[1], Marquis Elio[1], Rey Thomas[1], Hadjria Rafik[2] & Feyel Frédéric[12]

[1]Département de Génie Mécanique
École Normale Supérieure Paris-Saclay
4 avenue des sciences 91190 Gif sur Yvette
timothee.chastel@ens-paris-saclay.fr
elio.marquis@ens-paris-saclay.fr
thomas.rey@ens-paris-saclay.fr

[2]SAFRAN Tech – Département Sciences et Technologies du Numérique
Rue des jeunes Bois, Châteaufort, 78772 Magny-les-Hameaux Cedex-France
frederic.feyel@safrangroup.com
rafik.hadjria@safrangroup.com

KEYWORDS: deicing, ice detection, finite element modelling, piezoelectric, smart structures, features extraction

ABSTRACT

General Information

Currently, an aircraft de-icing system is a function that uses the hot air ejected by the engines without actually verifying the presence of ice at its surface. Consequently, this solution decreases the motor's efficiency. New engine architecture does not allow hot air to be re-routed to the inlet. The main focus of these engines being their efficiency the previous solution is no longer possible. A new solution based on multifunctional structures may allow to detect and deice at the same time. Piezoelectric transducer is a low consumption solution for this issue. This study analyses the possibility of using piezoelectric sensors to detect the presence of ice on an engine air entry.

A study of the pre-existing solutions was addressed based on piezoelectric transducers. Several solutions have been identified in the existing literature, some more relevant than the others. A first review of the existing solutions made by researchers allowed us to focus our analysis on specified methods **[1].** A first method to detect ice-formation relies on the analysis of ultrasonic shear horizontal guided waves **[2].** This article highlights several changes in the waves such as the frequencies of the different modes due to the presence of ice. It also highlighted changes in the phase and group velocities as well as the magnitude of the wave. Another method we retained is based on ultrasonic pulse-echo technique **[3].** On several occasions in different settings, the authors managed to link the time the wave took to go back and forth to the thickness of the ice. A last method focused on measuring the attenuation of ultrasonic waves to measure the thickness of the ice **[4].** The authors showed that the attenuation coefficient depended on the thickness and type of the ice thus allowing them to detect ice formation. The frequency used by the existing methods is definitely an issue for our application. The ice detection function being embedded into a dedicated onboard hardware, there is an issue to exploit high frequency range (higher than 100kHz). Thus, we chose to develop an ice detection algorithm that uses piezoelectric transducers in a low frequency range of aka 20kHz.

Our objective is twofold:

Part 1: A multiphysics finite element modelling and simulation of plate has been carried out with and without the presence of ice on the surface, using the software Comsol Multiphysics. The

simulation then focused on the real geometry of the air-entry to simulate signals sensed by the piezoelectric sensors. The goal of these simulations is to obtain the piezo-electric current/voltage response in the context of two piezo-electric waffles placed on both sides of an aluminum plate covered or not by ice. The entry is 24V, 0 to 20kHz frequency sweep with a 10Hz step. The observed output signal (Figure 2) matches the experimental data of both article **[5]** and SAFRAN sensor's lab experiments.

Part 2: The output data from simulation is used to extract some signal's feature. The selected features for this study are the frequency-domain transfer function, as well as the static capacitance (Figure 1), which allows us to check if the data is consistent as regards to the real configuration. An algorithm is developed to detect changes of these signals transfer functions thus detecting the presence of ice.
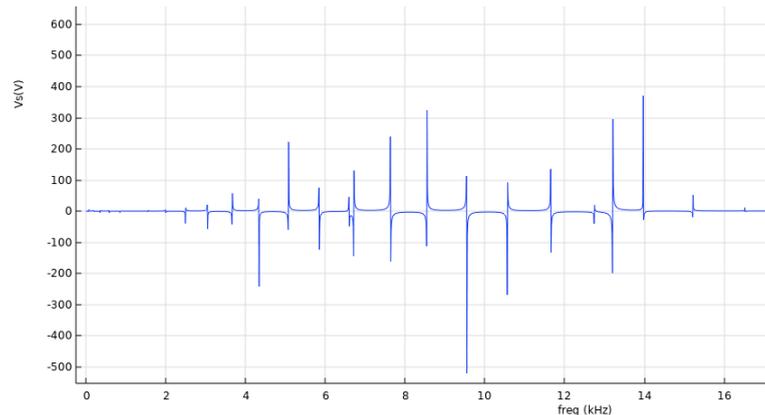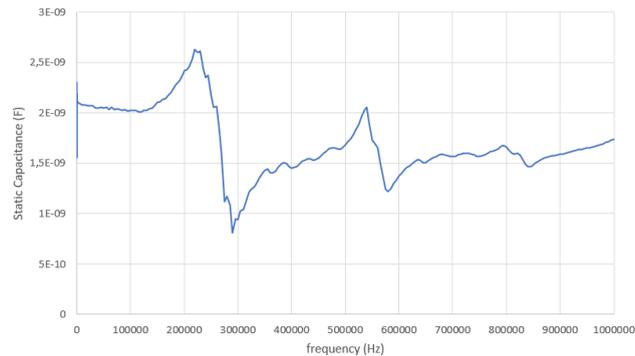

Figure 1: Output signal from Comsol

Figure 2: Determination of static capacitance

REFERENCES

[1] Homola, M.C., Nicklasson, P.J. and Sundsbø, P.A., 2006. Ice sensors for wind turbines. In: Cold regions science and technology ,46(2), pp.125-131 doi:10.1016/j.coldregions.2006.06.00

[2] H. Gao and J. L. Rose, Ice detection and classification on an aircraft wing with ultrasonic shear horizontal guided waves. In: IEEE Transactions on Ultrasonics, Ferroelectrics, and Frequency Control, vol. 56, no. 2, pp. 334-344, February 2009 doi: 10.1109/TUFFC.2009.1042

[3] R John Hansman and Mark S Kirby, Measurement of ice accretion using ultrasonic pulse-echo techniques. In: Journal of aircraft , 1985, Vol.22(6), p.530-535, doi/10.2514/3.45160

[4] LIU, Yang, BOND, Leonard J., et HU, Hui. Ultrasonic-attenuation-based technique for ice characterization pertinent to aircraft icing phenomena. In: AIAA Journal, 2017, vol. 55, no 5, p. 1602-1609. doi/10.2514/1.J055500

[5] ZHOU Su-Wei, LIANG Chen, ROGERS C. A. An impedance-based system modeling approach for induced strain actuator-driven structures. In: Journal of vibration and acoustics, July 1996, vol. 118, no 5, p. 323-331. doi: 10.1115/1.2888185
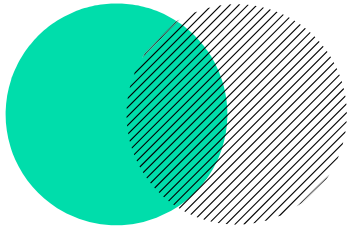
Construction of a homogenized mechanical model for a disordered optical fiber coil

L. KARAOUNI, A.BELLA, P.A. GUIDAULT

Simplified spot weld modeling by model reduction for the automotive industry

Karaouni Léa[*]**, Anass Bella**[†]**, Pierre-Alain Guidault**[◇]

Département de Génie Mécanique
Ecole Normale Supérieure Paris-Saclay
4 Avenue des Sciences, Gif-sur-Yvette, 91190, France
e-mail: {[*] lea.karaouni, [†] anass.bella}@ens-paris-saclay.fr

[◇] Université Paris-Saclay, CentraleSupélec, Ecole Normale Supérieure Paris-Saclay,
CNRS, LMPS-Laboratoire de Mécanique Paris-Saclay
Gif-sur-Yvette, 91190, France
e-mail: pierre-alain.guidault@ens-paris-saclay.fr

KEYWORDS: Finite element; Model reduction; Spot weld

ABSTRACT

Recently, automakers have been trying to make lighter cars in order to boost the aerodynamic performance of their vehicles. It so happens that spot welding is perfect to attach parts made of light materials together while building a car. Spot welding consists in using electric current to fuse together metal pieces without adding any additional material during the process. A car body contains about 4000-6000 spot welds and they are responsible for 80 % of fatigue failures on the car body. Yet, fatigue strength verification requires too fine finite elements meshes compared with car dimensions since spot welds' diameter is about 6 mm. There is therefore a need for simplified models of spot welds. However, existing models generally do not accurately reflect the fracture mechanisms involved in the fracture process of spot welds. Because of the apparent simplicity of the geometry of spot welds, they are often too simple and thus, inaccurate when a spot weld is close to sheet edges, a hole, or another spot weld for instance. Moreover, the identification of model parameters depends on the size of the finite elements used for the meshing of welded plates. Then, it is difficult not only to calibrate models in order to link plate models but also, to represent kinematics and local 3D effects induced by a spot weld. Indeed, existing models do not clearly account for the size of the spot weld's geometrical and mechanical zone of influence [1]. The aim of this study is to propose a spot weld model for plate model connection that is accurate enough for a wider range of applications (fatigue, static, dynamics) with no mesh dependency and that enables rapid reconstruction of 3D solutions in the spot weld for fatigue analysis.

Methodology and results

In this study, a simplified model of spot weld with reduced basis technique is proposed. First, the following method is developed for the half of a spot weld which corresponds to the upper plate and half of the spot weld core. Relevant 3D solutions that welded sheets can encountered were collected in spot weld's vicinity and subsequently a load basis and associated plate modes were generated. Then, a reduced basis is constructed from these

plate solutions by POD (Proper Orthogonal Decomposition) in the sense of the energetic norm. After the construction of the simplified model by plate strain energy equivalence, it was connected kinematically to its environment by writing the displacement continuity in a weak sense. For the purpose of validating our spot weld model, several elementary tests were conducted on the upper half of the model. The 3D model (Figure 1a) is clamped on the cross section of the weld core and various loadings were applied on the edge of the upper plate. Prescribed translation displacement $\mathbf{U_d}$ and rotation $\mathbf{\Omega_d}$ are defined at a master node and plate solution is constructed from 3D solution. It was found that the 3D effects that the plate model can not represent are localized in the vicinity of the spot weld core. Thus, it is important to carefully choose the selection radius when constructing the reduced basis in order to represent accurately the geometric and mechanical zone of action of the spot weld. It was found that the radius of influence should be slightly bigger than the actual radius of the spot weld [2]. It was also shown that the simplified model can correctly represent the clamping effect induced by the spot weld (Figure 1b). The deformed shape is plotted in Figure 1 for $\mathbf{U_d}.\mathbf{z} = 1\,mm$, which is a load present in the reduced basis.
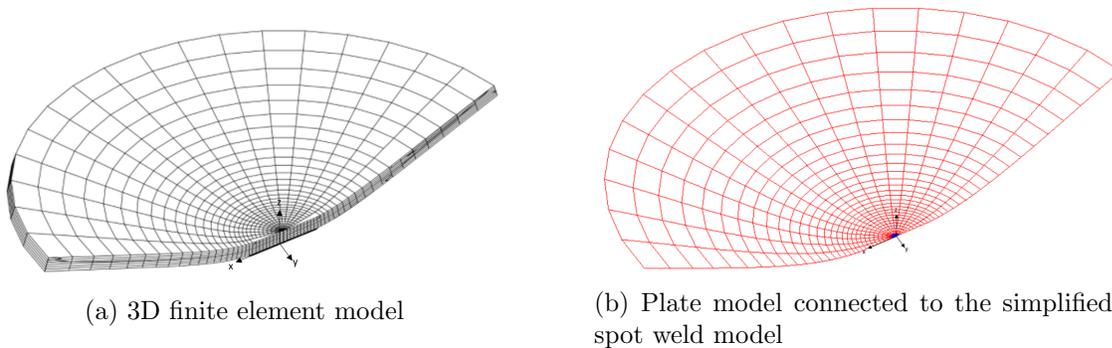

(a) 3D finite element model

(b) Plate model connected to the simplified spot weld model

Figure 1: Deformed shape for 3D model and simplified model with $\mathbf{U_d}.\mathbf{z} = 1\,mm$

Conclusion and future work

These findings suggest that the simplified model responds accurately to elementary loads and that the methodology can be easily generalized to every load case. However, they also pave the way for further investigations. Indeed, the possibility of automatic model enrichment is yet to be studied.

REFERENCES

[1] P.-A. Guidault *Sur les interfaces en mécanique non-linéaire des structures.* Habilitation à diriger des recherches, Université Paris-Saclay, 2020.

[2] F. Mainnemare *Modélisation du point de soudure électrique pour la tenue en service des structures automobiles.* Thèse de doctorat, Université Paris-Saclay, 2021.
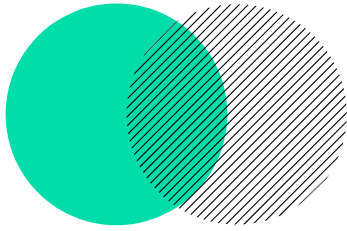
Numerical simulation of the propagation of a crack in mixed modes I + III

P. GOUEFFON, A. HEMBERT, M. SUSINI, Y.GUILHEM

Numerical simulation of the propagation of a crack in mixed modes I + III

Pierre GOUEFFON$^{\heartsuit}$, **Arthur HEMBERT**$^{\diamondsuit}$, **Maxime SUSINI**$^{\spadesuit}$, **Yoann GUILHEM**$^{\clubsuit}$

$^{\heartsuit}$ pierre.goueffon@ens-paris-saclay.fr $^{\diamondsuit}$ arthur.hembert@ens-paris-saclay.fr

$^{\spadesuit}$ maxime.susini@ens-paris-saclay.fr $^{\clubsuit}$ yoann.guilhem@ens-paris-saclay.fr

$^{\heartsuit\diamondsuit\spadesuit\clubsuit}$ Department of Mechanical Engineering
Ecole Normale Supérieure Paris-Saclay
4 avenue des Sciences, 91190 Gif-Sur-Yvette

KEYWORDS: crack propagation ; mixed modes ; mixity ratio ; Abaqus ;

ABSTRACT

Context

One of the prime challenges of the aeronautical industry is the reduction of greenhouse gases, which can be achieved through a reduction of component weights. Under nominal load, components are subject to fatigue, leading to the appearance of cracks, which can have catastrophic safety implications. In these circumstances, Safran Aerobooster is developing a new assembly process in which the blade is directly welded instead of bolted onto the disc. However, the continuity between these two components offers a possible path for cracks to propagate to the disc, which is a critical safety concern. Hence, it is vital to study the propagation of these cracks.

Figure 1: Specimen and loads

The goal of this research is to numerically explore the propagation of cracks in mixed fracture modes I + III, used to model typical load cases for the blade. To this effect, starting from a specimen shape inspired from [1], numerical simulations were carried out to explore the influence of various test parameters (actuator position, displacement or stress test, antisymmetric loading...) and study their influence on output variables, such as stress intensity factors or mixity ratio [2, 3].

Methods

Numerical simulations were carried out in Abaqus (a software suite for finite element analysis) using an elastic model. Indeed, plasticity was assumed to be confined in the vicinity of the crack, and having no influence on the global behaviour. What is more, stress intensity factors are computed via interaction integrals, which is a routine integrated in Abaqus. To automate the simulations, a Python script was written in order to command Abaqus and easily modify entry variables.

Due to the dynamic limitations of Abaqus, the simulations were carried out by applying loads on a set of discrete specimens each with a fixed crack length (Figure 1). For all simulations, crack propagation
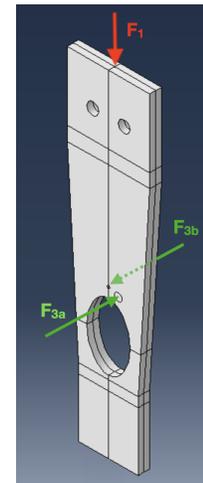
was supposed straight, a strong hypothesis given the loads applied on the specimen (the crack may twist for instance).

Initial implementation of mode III fracture, with a lateral load applied on only one side, showed a bulging phenomenon. To limit this, an antisymmetric load on the other side was introduced (see Figure 2), with an added benefit that it smoothed the mode I stress intensity factor (SIF) along the crack front.

Results

For the needs of the experiment two cases of evolution for the mixity ratio according to crack length were wanted. In the first case, the mixity ratio would be increasing with the crack length, which was achieved through constant loading in the longitudinal and lateral axis (Figure 3). In the second case, the aim was to have a constant mixity ratio, which could not be obtained. Some possible paths to explore include constant displacement along the two axis, a mix of constant displacement and load, or varying displacement and load conditions, although the latter seem rather tedious to implement practically.

Further work may focus on the changing crack plane which can have a major impact on the safety of the new assembly process.
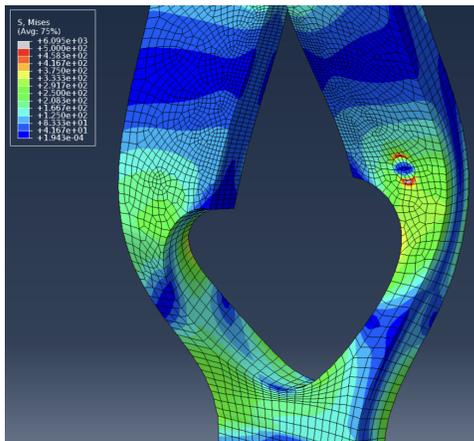
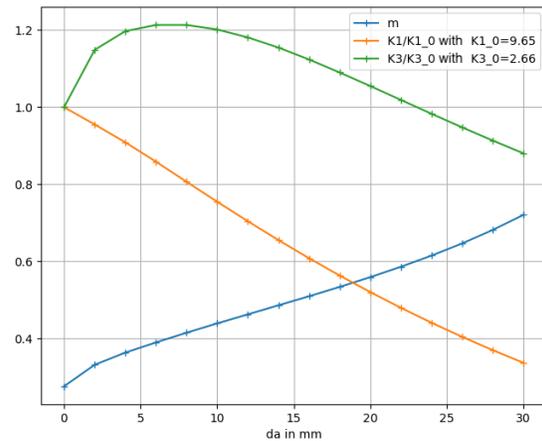**Figure 2**: Deformed specimen and Von Mises stress

Figure 3: Mixity ratio (m) and dimensionless SIF (K1 and K3) according to crack length

REFERENCES

[1] C. Mary; C. Cluzel; R.F. De Moura Pinho et. al. Patent No.: US 9,423,330 B2 Date of Patent: 2016

[2] G. R. Irwin. Analysis of stresses and strains near the end of a crack traversing a plate. Journal of Applied Mechanics, 24(3):361–364, 1957. DOI : 10.1115/1.4011547

[3] F. Fremy; S. Pommier; E. Galenne; S. Courtin. A scaling approach to model history effects in fatigue crack growth under mixed mode I + II + III loading conditions for a 316L stainless steel. International Journal of Fatigue vol.42, Sept.2012 pp.207-216, ISSN 0142-1123
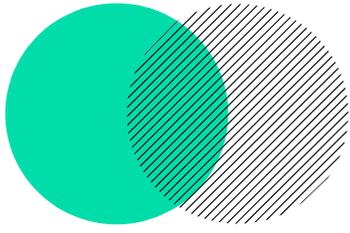
Fracture mechanic of architectured materials

C. ROGIER – C. LELONG – F. DAGHIA

Tomographic Monitoring of Cracking in 3D Printed Polycarbonate and Acrylonitrile-Butadiene-Styrene Specimens

Q. Charmoillaux[*], **L. Person**[*], **B. Smaniotto**[*,◇], **R. Vargas**[◇], **F. Hild**[◇]

École Normale Supérieure Paris-Saclay
4 avenue des Sciences, 91190 Gif-sur-Yvette, France
e-mail:{quentin.charmoillaux, lucas.person, benjamin.smaniotto, rafael.vargas_maginador,
francois.hild}@ens-paris-saclay.fr
[*]DER Génie Mécanique
[◇]LMPS - Laboratoire de Mécanique Paris-Saclay

KEYWORDS: Additive manufacturing; cracking; digital volume correlation; energy release rate; tomograph

ABSTRACT

Additive manufacturing is being used more and more in the industrial sector [3]. It has recently come up with novel materials, of which the behavior widely remains to be determined due to anisotropic and heterogeneous features, and a strong dependence on the printing pattern [1]. Image correlation and tomography have been proven to be particularly useful tools to study cracking [4]. The aim of this work is to observe and quantify crack propagation in acrylonitrile-butadiene-styrene (ABS) and polycarbonate (PC) parts printed by fused deposition modeling with a [0°/90°] layup when monitored in an X-ray tomograph. The captured scans were used to measure displacement fields through digital volume correlation (DVC).

Methods

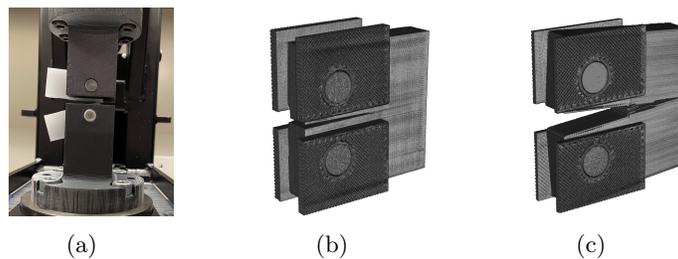Two compact tension samples were tested in situ (in an X-ray tomograph, figure 1) until failure.

Figure 1: (a) In situ loading device after failure. Scanned PC (b) and ABS (c) samples just before failure

To obtain 3D images, it was necessary to record radiographs for 900 angular positions of the sample with respect to the detector. A 60 µm/voxel resolution was reached in the reconstructed images whose size was $250 \times 925 \times 925$ vx, figure 1(b,c). The captured scans were used to measure displacement fields through digital volume correlation. It is based on the assumption of gray level conservation for every material point. The sought displacement minimizes the root mean square residual [2]. In order to perform DVC analyses, a coarse mesh was first used, then adapted refined meshes were constructed for each material. Very large displacements occurred in the ABS sample (figure 2(c)), contrary to the PC specimen (figure2(b)). Concerning the latter, a "pacman"-like mesh was created to measure the displacement fields in the crack front vicinity. For ABS, the coarse mesh was constructed on a 2D section for which the in-plane displacement fields were measured via digital image correlation. From the profile of maximum gray level residuals, the cracked line was obtained, and a new 2D mesh was constructed with GMSH. This 2D mesh was subsequently extruded along the thickness of the sample. Similarly, the 2D displacements were extruded along the same direction and used as initialization of each DVC calculation.
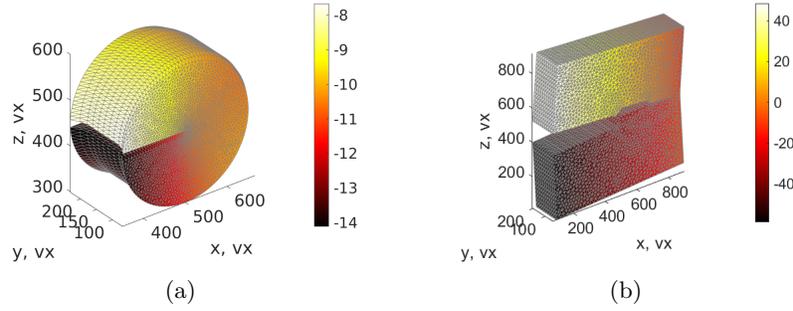
Figure 2: Vertical (z) displacement fields expressed in vx for the PC (a) and ABS (b) samples

Results

For the PC sample, the displacement field close to the crack tip was projected onto Williams' series [5] via least squares minimization, which led to the stress intensity factors K_I, K_{II}, K_{III}, and the energy released rate G (figure 3(a)) for each loading step. Figure 3(b) shows the nodal gray level residuals for the last scan of the ABS sample. Except for the immediate vicinity of the cracked surface, they remained very small, thereby proving that the DVC calculations were successful. With the present initialization strategy, only 9 iterations were needed to capture displacement amplitudes of the order of 60 vx (figure 2(b)), which proves its usefulness and robustness.
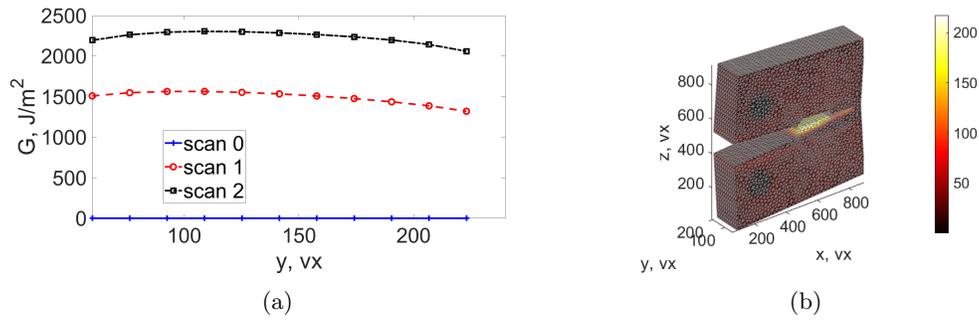

Figure 3: Energy release rate profiles along the depth of the PC sample for the 3 scans (a). Gray level residuals for the last scan of the ABS sample (b).

In addition, qualitative observations suggest that the printing pattern plays a role on the crack path shape, which followed layer interfaces. Last, PC was more brittle than ABS that deformed plastically. Thus, this study contributed to the understanding of cracking and sizing of additive manufactured parts. Nonetheless, further investigations should be conducted, for example with various printing parameters and sample geometries.

REFERENCES

[1] T. Corre and V. Lazarus. Kinked crack paths in polycarbonate samples printed by fused deposition modelling using criss-cross patterns. *International Journal of Fracture*, 230:19–31, 2020.

[2] F. Hild and S. Roux. Digital image correlation. In P. Rastogi and E. Hacks, editors, *Optical Methods for Solid Mechanics. A Full-Field Approach*, pages 183–228. 2012.

[3] T. D. Ngo, A. Kashani, G. Imbalzano, K. T.Q. Nguyen, and D. Hui. Additive manufacturing (3D printing): A review of materials, methods, applications and challenges. *Composites Part B: Engineering*, 143:172–196, 2018.

[4] M. A. Sutton, J. J. Orteu, and H. Schreier. Image Correlation for Shape, Motion and Deformation Measurements. *Springer*, pages 205–221, 2009.

[5] M. L. Williams. On the Stress Distribution at the Base of a Stationary Crack. *Journal of Applied Mechanics*, 24(1):109–114, 1957.
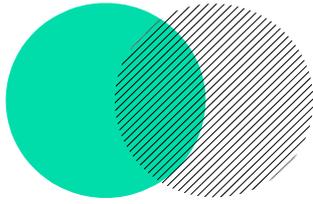
Measurement of the deformations of an optical fibre coil under thermal loading

C. CHEDOZEAU, Y.DUBREUIL, Q.JAVEY, K.LAVERNHE, F.LOUF

Measurement of the deformations of an optical fibre coil under thermal loading

Students

Clément Chedozeau, Yvan Dubreuil, Quentin Javey
DER Génie Mécanique, ENS Paris-Saclay
clement.chedozeau@ens-paris-saclay.fr
yvan.dubreuil@ens-paris-saclay.fr
quentin.javey@ens-paris-saclay.fr

Supervisors

Karine Lavernhe, François Louf
LMPS, ENS Paris-Saclay
karine.lavernhe@ens-paris-saclay.fr
francois.louf@ens-paris-saclay.fr

ABSTRACT

Fibre Optic Gyroscopes (FOG) are the most accurate gyroscopes used in inertial measurement units with an accuracy over $0,01°$/hour, far superior to other gyroscopes that have, at most, a precision of $1°$/hour. When aiming to bring a submarine from the west coast of France to the east coast of the United States without using the GPS, gyroscopes as well as accelerometers need to be as accurate as possible.

FOGs are based on the Sagnac effect, the sensitivity of which lies in the enclosed area. To maximise this area the fibre is wound into an orthocyclic quadrupolar winding. For optical fibres, the refractive index depends on the local strain and therefore deformations of the coil structure, especially inertial units which are subject to significant temperature variations [1]. It is therefore necessary to study the response of the coil to thermal loading in order to optimise the type of winding and materials that could reduce the effect of thermal loading.

However, coils are made of fibres and epoxy glue whose thermal characteristics were only studied separately in previous studies. The coil is heterogeneous, anisotropic, whose mechanical properties depend on the temperature. The studies were focused on the optimisation of the winding type of the coil in regards to minimising the effects of thermal loading [2]. Recently, work carried out in a thesis made it possible to develop models based on the finite element method to predict strain caused by thermal loading [3]. These models still require to be validated on the basis of experimental results. The objective of the envisaged study is to carry out a test campaign to estimate the deformations undergone by a coil under thermal loading. This study could help anticipate the manufacture and design of future coils as well as the materials used, minimising deformations induced by thermal loading.

Digital image correlation (DIC) [4] and strain gauges were used. A first test was carried out on an aluminium ring to develop the correlation and the measurement and heating protocol. The advantage is that the reaction of aluminium to thermal loading is already known. We used a self made thermal chamber (figure 1) to have the desired temperature both in uniformity and stability in the ring. We used both strain gauges and image correlation to have a strain map of the coil and confirm the results at specific points. An autocorrelation was also performed to assess the measurement noise for the correlation.
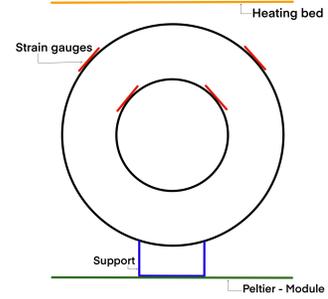
Figure 1: Thermal Chamber
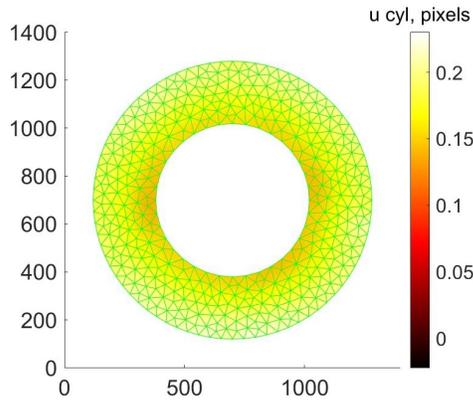
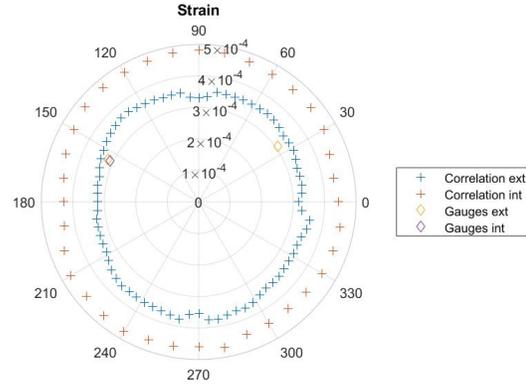**Figure 2**: Radial displacement at 50°C (starting at $T_{ini} = 25$°C)

Figure 3: Orthoradial strain on interior and exterior faces at 50°C (starting at $T_{ini} = 25$°C)

The digital image correlation results gives an axisymmetric radial displacement field increasing with radius (figure 2) which is consistent with an isotropic homogeneous materials submitted to an homogeneous thermal loading. In addition, there is an order of magnitude difference between the radial and orthoradial displacement which seems consistent. The average of the thermal dilatation coefficient is $18.7\mu K^{-1}$ ($23\mu K^{-1}$ for common aluminium). It is also noted that the correlation and strain gauges give close results for the orthoradial strain on the external face (figure 3). The strain should be constant on the whole ring as the gauges shows. The different results obtained by correlation require additional studies. After the validation of the protocol on the aluminium ring, we can experiment it on the FOG. To ensure that the temperature is the same in the whole ring, we used another FOG coil which is instrumented with thermocouples at its core. The first result from a simple model was that the coil would both expand to the interior and the exterior because of the great difference between the coefficient of thermal expansion of the fibre and the glue. Further experiments need to be carried out to fully characterise the behaviour of the coil.

REFERENCES

[1] D. M. Shupe. Thermally induced nonreciprocity in the fibre-optic interferometer. *Appl. Opt.* **Vol**: 19, pp. 654-655, 1980.

[2] F. Mohr. Thermooptically Induced Bias Drift in Fibre Optical Sagnac Interferometers. *Journal of Lightwave Technology* **Vol**: 14 issue 1, pp. 27-41, 1996.

[3] J. Pillon. . *PhD Thesis 2022*, Université Paris-Saclay, in French.

[4] G. Besnard, F. Hild, S. Roux. "Finite-Element" Displacement Fields Analysis from Digital Images: Application to Portevin–Le Châtelier Bands. *Experimental Mechanics* **Vol**: 46, pp. 789–803, 2006.
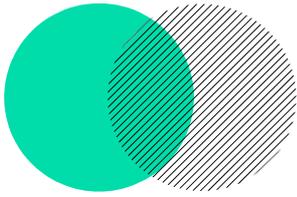
Monitoring of a laser powder bed fusion using a thermal camera

S.MEKSAVAN, L.BECHU, N.MULLER

école
normale
supérieure
paris—saclay

Monitoring of a laser powder bed fusion using a thermal camera

Simon MEKSAVAN, Louis BECHU, Nicolas MULLER

Department of mechanical engineering (DGM)
ENS Paris-Saclay, 4 Av. des Sciences, 91190 Gif-sur-Yvette, France
e-mail: {simon.meksavan, louis.bechu, nicolas.muller}@ens-paris-saclay.fr

KEYWORDS : Additive manufacturing, laser powder bed fusion, in-situ monitoring, IR camera, material health, experimental design

ABSTRACT

General information

Additive Manufacturing and especially the Laser Powder Bed Fusion technology is generally used to manufacture complex parts, layer by layer. Although this technology has its own advantages over others technologies, some drawbacks need to be frowned upon. These issues mostly have a thermal origin and lead internal defects located inside printed parts.
Indeed, the parts melted powder is inhomogeneous due to thermal inconsistency during the printing process throughout the part[1]. Previous researches show that during the printing, several parts areas possess different cooling rates, revealing a thermal discrepancy in the manufactured product[2]. These observations were made by using a thermal camera, calibrated with blackbody calibration[3]. Although a thermal cartography of cooling rate layer by layer was previously made[1], at the moment, no links were made between in-parts defects and cooling rates, which could be helpful to spot thermal relative defects on a manufactured part.

Method and results

The main objective of this study is to elaborate a cartography of thermal gradient layer by layer in order to point out defects in the final product, but due to hardware limitations only a relative one is possible to achieve. Defects detected through the cartography are compared with defects located using simulations.
As such, several recipes of manufacturing, including different shapes, were created. During the process, regularly timed-spaced IR snapshots were taken using the considered IR camera. Images post-processing was made using MATLAB 2021b developing environment and leads to a cooling rates 3D-map of the printed part by stacking results from each layer.
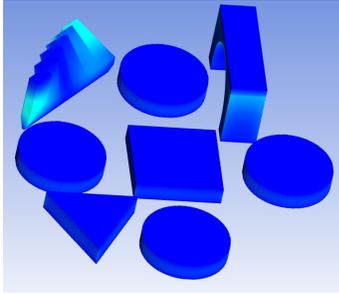Identified patterns were correlated with Ansys an Altair software thermomecanical simulations.

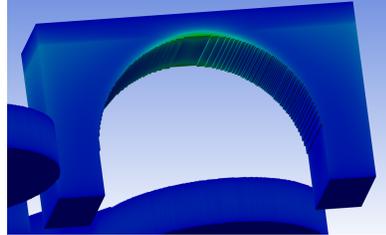**Figure 1**: Thermal simulation of parts manufactured with Laser Powder Bed Fusion technology by Ansys

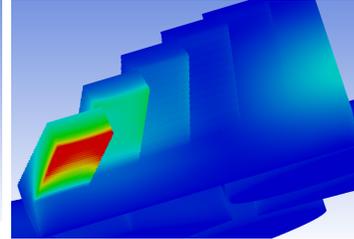

Figure 2: Focus on the bridge


Figure 3: Focus on the angle

Conclusion

Confrontations between simulations and acquisition 3D model, show that corners and thin areas of the printed parts are affected by the cooling rate (which can be linked to local maximum temperature) during the process. Moreover, shapes that are more inclined to present defects were identified thanks to simulations.

The post-processing uses simple operations only and it could possibly be implemented in the CNC machine allowing a in real time monitoring. Another solution in order to prevent defects would be to modify the recipe in using data from the simulations.

An observation of the horizontal linearity of the powder level using a laser could also be implemented, hence focusing on the link between thermal discrepancy and powder thickness, in order to make defects even easier to spot.

REFERENCES

[1] Jarred C. Heigel, Eric Whitenton. *Measurement of thermal processing variability in powder bed fusion.* Engineering Laboratory National Institute of Standards and Technology Gaithersburg, MD, USA.

[2] Eric Whitenton, Brandon Lane, Shawn Moylan . *Multiple Sensor Detection of Process Phenomena in Laser Powder Bed Fusion*, Proceedings of SPIE - The International Society for Optical Engineering, May 2016.

[3] Brandon Lane, Eric Whitenton. *Calibration and Measurement Procedures for a High Magnification Thermal Camera*, National Institute of Standards and Technology, January 2016.
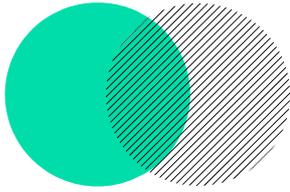
Experimental study of the buckling of architectured
materials under biaxial
compressionor

M.HERAULT-ARDXOUIN, B.LESCANNE
M.WANGERMEZ, M.PONCELET

école
normale
supérieure
paris—saclay

Experimental study of the buckling of architectured materials under biaxial compression

M.Hérault-Ardouin[*], **B.Lescanne**[*], **M.Wangermez**[†], **M.Poncelet**[†]

[*] Département de génie mécanique
Ecole Normale Superieure Paris-Saclay
4 Avenue des Sciences, 91190 Gif-sur-Yvette
[*]corresponding author e-mail: balthazar.lescanne@ens-paris-saclay.fr

[†] Laboratoire de Mécanique Paris-Saclay
Université Paris-Saclay
4 Avenue des Sciences, 91190 Gif-sur-Yvette

KEYWORDS: Architectured materials; biaxial compression; buckling; test machine.

ABSTRACT

Context and introduction

Because of their particular internal structures combining matter and void, architectured materials can have different intrinsic properties (e.g. stiffness anisotropy or specific yield stress) than bulk materials. Such materials present these uncommon behaviors because of their cell structures, made of slender beams or walls. Due to this architectured materials tend to buckle with "internal modes".

The numerical model of C.Combescure [1] predicts the appearance of different internal buckling modes. The goal of this project is to control and better the understanding of the biaxial compression machine built previously to confront this numerical model with biaxial compression experiments. Previous researchers, like S.D.Papka and S. Kyriakides [2] or S. Shan et al. [3], also worked on biaxial crushing test machines, but, their machines did not allow the measurements of the forces applied to the sample. Due to the intrinsic difficulties of biaxial compression kinematic, the force distribution is, moreover, highly likely to be heterogenous. Consequently the present work also investigates this point.

Biaxial compression machine

We started from a machine which was designed for a specimen size of $170mm \times 170mm$ and a 50% compaction ratio. The first goal was to adapt a python 3.8 rogram made for another machine. With 4 load cells on the machine it is possible to measure the tangential and normal forces as well as the application point during the experiments by resolving a linear system predetermined by calibrating the machine with masses. The question of the degree of freedom at the boundary was raised because due to the geometry of honeycombs on two sides cells are free to rotate while on the two others they can only slide. We thus designed two kind of specimen one only with honeycombs and the other with stands on the two sides where the cells can rotate. Finally teflons adhesive was used to reduce the friction and improve force distribution homogeneity
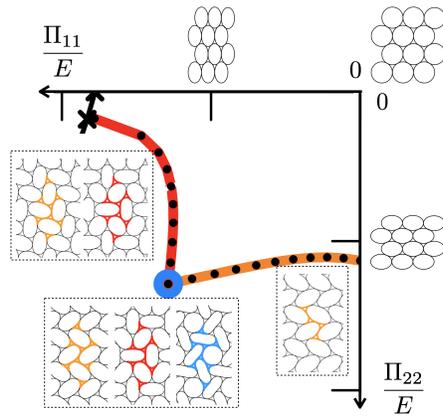
(a) C.Combescure model
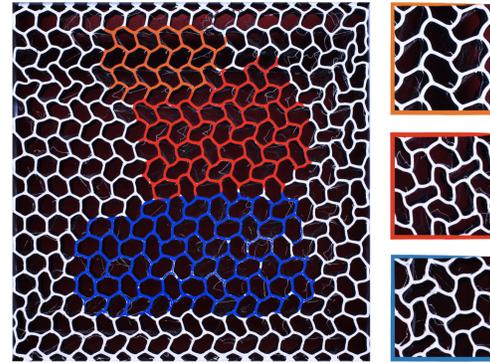
(b) Experimentals results

Key Results and interpretations

Simulations using CASTEM on an isotropic bulk material showed that the normal force should change along each side of the machine due to the peculiars boundary conditions. Moreover we noticed that tangentials forces are not negligible even with the teflon covered surfaces. Another issue is the poor quality of FDM 3D printing of the TPU specimen with problems such as wall thickness or TPU thread remaining. Eventually the question of the architectured material pattern itself is raised. In fact it is difficult to find a relevant mode to study because some are much more sensitive to multiaxiality or boundary conditions than others. For hexagonal cells we obtained the results on figure (b) where different patterns appeared simultaneously on the specimen due to the heterogenous forces. In theory circular cells buckling is independant of the forces and only blue pattern appear.

REFERENCES

[1] C. Combescure, P. Henry, R.S. Elliott. Post-bifurcation and stability of a finitely strained hexagonal honeycomb subjected to equi-biaxial in-plane loading. *Int. J. of Solids and Structures* .**88(89)**: 296-318, 2016.

[2] S.D. Papka, S. Kyriakides Biaxial crushing of honeycombs - Part I: Experiments. *Int. J. of Solids and Structures* **36(29)**: 4367-4396, 1999.

[3] S. Shan et al. Harnessing Multiple Folding Mechanisms in Soft Periodic Structures for Tunable Control of Elastic Waves. *Adv. Funct. Mater.* **24(31)**: 4935-4942, 2014.
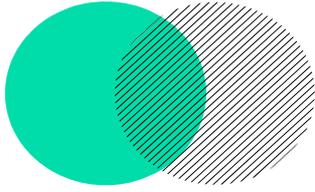
Parametric Optimisation of Scanning Patterns in Laser Powder Bed Fusion (L-PBF)

M. RIERA, E. ROBILLARD, C.TOURNIER

Parametric Optimisation of Scanning Patterns in Laser Powder Bed Fusion (L-PBF)

M. Riera*, E. Robillard*, C. Tournier◇

Université Paris-Saclay
Ecole normale supérieure Paris-Saclay
* ◇ Department of Mechanical Engineering
◇LURPA
4, avenue des Sciences, 91190 Gif-sur-Yvette, France
{mathis.riera ; eva.robillard ; christophe.tournier}@ens-paris-saclay.fr

KEYWORDS: Additive Manufacturing, Genetic Optimisation, Scanning Strategy, Heat Conduction.

ABSTRACT

General Context

Laser powder bed fusion (L-PBF) is an additive manufacturing process that produces parts layer-by-layer from a numerical model, in which the scanning strategy is critical for both production rates and the physical and mechanical properties (microstructure, residual stress). Previous research has focused on improving process productivity while enhancing conventional patterns (zigzag and helix) [1]. This has led to new scanning strategies and patterns obtained by structural optimisation [2]. The aim of this study is to define a parameterised geometric model of patterns suitable for different shapes and materials.

Methods

The objective is to obtain the shortest pattern in length while melting the powder in a predefined area with the least amount of overheating. This nonlinear parametric optimisation problem is solved using a genetic optimisation taken from the Matlab Toolbox "Global Optimization". Paired with a flash based thermal simulation of scanning paths [3] (the "Flash" method), it makes it possible to adjust the parameters of the pattern while complying with thermal constraints and laser characteristics set constant (scanning speed and power). These constraints are modelled by the minimisation of a criteria (Equation 1) regarding the temperatures both inside and outside the considered area. The study initiates from the parameterisation of complex patterns (Figure 1) on which multiple simplifications are brought up considering symmetry and redundancy.

$$Crit = a \left(\sum_{i \in \Sigma} \left([T_f - T_i]^+ \right)^\alpha \right)^{\frac{1}{\alpha}} + b \left(\sum_{i \in \Sigma} \left([T_i - T_c]^+ \right)^\beta \right)^{\frac{1}{\beta}} + c \left(\sum_{i \in \bar{\Sigma}} \left([T_i - T_f]^+ \right)^\gamma \right)^{\frac{1}{\gamma}} \quad (1)$$

$$Crit = \frac{P_{laser} * L_{traj}}{v * S_{domain}} \quad (2)$$
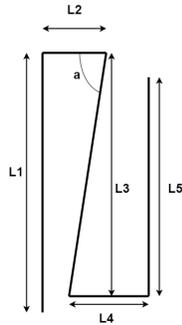
Figure 1:
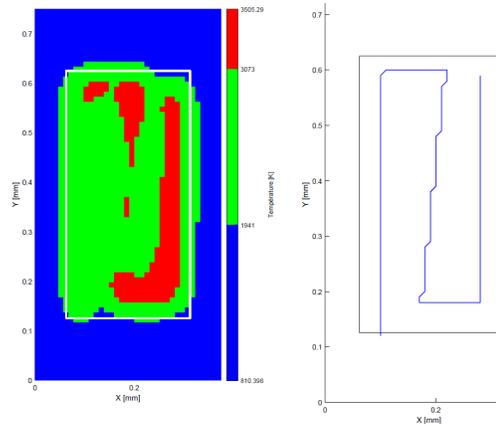Parameterised
zigzag pattern

Figure 2: Heat map and final shape of
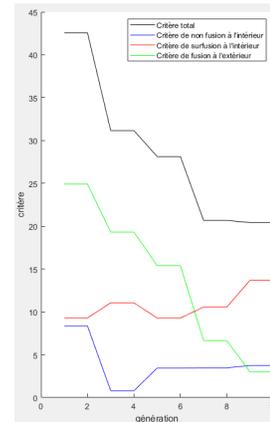the optimised zigzag

Figure 3:
Convergence of the
optimisation

Results

This method enables the optimisation of the common pattern of a zigzag scan (Figure 1) by the introduction of an angle to benefit from the preheating of the previous scanning line. It has been executed on several patterns, and energetic performance criteria (Equation 2) have been established for comparison with conventional patterns. The optimisation conducted on the zigzag scan has led to the appearance of a slight angle according to the expectations in terms of preheating in the area (Figure 2 and 3). Other optimisations were studied starting from patterns of previous structure optimisations [2].

Further work

Considering only the length of a pattern when evaluating time efficiency may be insufficient. An extended model that includes speed variations of the laser would be of better accuracy. Furthermore, the study has mostly been carried out on titanium, but other materials could be considered to ensure a more general approach. Finally, an experimental approach is yet to be conducted to validate that using such patterns is not made at the cost of the part quality.

REFERENCES

[1] H. Jia, H. Sun, H. Wang, Y. Wu, and H. Wang, Scanning strategy in selective laser melting (slm): a review, *The International Journal of Advanced Manufacturing Technology*, 113(9):2413-2435, 2021. https://doi.org/10.1007/s00170-021-06810-3.

[2] M. Boissier, G. Allaire, and C. Tournier, Time dependent scanning path optimization for the powder bed fusion additive manufacturing process, *Computer-Aided Design*, 142:103122, 2022. https://doi.org/10.1016/j.cad.2021.103122

[3] K. Ettaieb, S. Lavernhe and C. Tournier, A flash-based thermal simulation of scanning paths in LPBF additive manufacturing, *Rapid Prototyping Journal*, 27(4): 720-734, 2021. https://doi.org/10.1108/RPJ-04-2020-0086